

# Materials screening for attenuating embedded phase-shift photoblanks for DUV and 193 nm photolithography

P. F. Carcia, R. H. French, K. Sharp, J. S. Meth, B. W. Smith<sup>#</sup>

DuPont Co. Central Research, Experimental Station, Wilmington, DE 19880-0356

<sup>#</sup>Rochester Institute of Technology, Microelectronic Engineering, Rochester, NY 14623-0887

## ABSTRACT

We surveyed more than 150 different materials as candidates for optically tunable (at 248 nm and 193 nm), attenuating embedded phase-shift masks. Multicomponent materials with four distinct microstructures: (1) composites, (2) cermets, (3) multilayers, and (4) copolymers, where one component was optically clear at the application wavelength and the other component more optically absorbing, provided a systematic approach for adjusting the needed optical properties: specifically, optical transmission and  $\pi$ -phase-shift. From evaluation of optical properties and other mask manufacturability issues, including chemical and radiation durability, etch selectivity, alignment and inspection properties, film stress and adhesion, we identified promising nitride and oxide materials based on  $MN_x$ -AlN (M=Cr, Mo, W,...) and  $M'O_y$ -RuO<sub>2</sub> (M'=Al, Hf, Zr...) as well as promising polymers.

Keywords: microlithography, photomasks, phase shift masks, attenuating embedded phase shifter

## 1. INTRODUCTION

A phase-shift mask<sup>1-6</sup> is an optical enhancement tool that allows printing smaller circuit features with existing lithography systems, without reducing depth of focus. Although there are a number of different types<sup>2,3</sup> of phase-shift masks, attenuating embedded phase-shifters (AES)<sup>2-7</sup>, that are partially transmitting, are especially attractive because design and processing of the reticle are simplified. To exploit these advantages in DUV and 193 nm lithographies, it is essential to develop the next generation of phase-shift masks. This paper describes results of a broad based literature search and materials screening effort to identify and evaluate versatile materials families for attenuating embedded shifters for DUV and 193 nm. As summarized in Table 1, mask requirements include 180° phase shift at DUV and 193 nm with transmissivity 4-10%, etch selectivity relative to the quartz substrate and photoresist, as well as chemical and radiation durability. And the goal is to achieve these properties with a single material's family that can be tuned to perform at both wavelengths.

Table 1. Target DUV/193 AES Material Specifications	
Phase Shift at 248 and 193 nm	180° +/- 5°
Transmission at 238 and 193 nm	4 - 10 %
Reflectivity at 249 and 193 nm	< 15%
Transmission at 488 nm	< 40%
Resistivity	< 10 <sup>6</sup> ohms/square
Etch Selectivity to Quartz	2:1
Etch Selectivity to Resist	2:1
Chemical Durability	>2 hr. in 90° C H <sub>2</sub> SO <sub>4</sub> /H <sub>2</sub> O <sub>2</sub>
Radiation Durability	No degradation in Opt. Prop.
Adhesion to Quartz	ASTM Crosshatch tape test

After surveying the available literature, we concluded that multi-component materials would best satisfy the demanding optical properties for new phase shift masks. One component would be optically clear with a band gap > 6 eV, and the other component would be absorbing, such as a metal, metal-nitride or -oxide. Table 2 lists most of the binary compounds that are optically "clear" at DUV. In this study we deliberately omitted Si-based materials, because we

P. F. Carcia, R. H. French, K. Sharp, J. S. Meth, B. W. Smith, "Materials Screening for Attenuating Embedded Phase-Shift Photoblanks for DUV and 193 nm Photolithography", **16th Annual BACUS Symposium on Photomask Technology and Management, SPIE Vol. 2884**, Edited by G. V. Shelden, J. A. Reynolds, 255-63, (1996).

anticipated that they would have inferior etch selectivity to the quartz substrate. And focusing only on candidates that also had prospects for attractive etch characteristics and chemical durability, we systematically synthesized multicomponent candidates with four distinct microstructures: (1) composites<sup>5</sup> (2) cermet<sup>8,9</sup>, (3) multilayers<sup>10</sup>, and (4) copolymers<sup>11</sup>.

<b>BN</b>	<b>B<sub>2</sub>O<sub>3</sub></b>	<b>SiO<sub>2</sub></b>	<b>BeO</b>	
<b>AlN</b>	<b>Al<sub>2</sub>O<sub>3</sub></b>	<b>GeO<sub>2</sub></b>	<b>MgO</b>	<b>MgF<sub>2</sub></b>
<b>Si<sub>3</sub>N<sub>4</sub></b>	<b>Y<sub>2</sub>O<sub>3</sub></b>	<b>ZrO<sub>2</sub></b>	<b>CaO</b>	<b>CaF<sub>2</sub></b>
<b>C</b>	<b>Cr<sub>2</sub>O<sub>3</sub></b>	<b>HfO<sub>2</sub></b>	<b>SrO</b>	<b>SrF<sub>2</sub></b>
		<b>CeO<sub>2</sub></b>	<b>BaO</b>	<b>BaF<sub>2</sub></b>
<i>polymers</i>				<i>alkali halides</i>

**Composites** are the analog of metal alloys. They are comprised of an atomic or molecular mixture of at least two components, one of which is optically transmitting while the other component is optically more opaque. This mixture can be homogeneous or inhomogeneous. "MoOSiN", proposed as a DUV phase-shift mask<sup>12</sup>, is an example of a complex composite consisting of MoO<sub>3</sub>-Si<sub>3</sub>N<sub>4</sub>-SiO<sub>2</sub>-MoN, made by sputtering Mo-Si reactively in Ar+N<sub>2</sub>+O<sub>2</sub>.

**Cermet**s are comprised of an elemental metal dispersed in a ceramic matrix. M-AlN, where M refers to a small concentration of metal homogeneously or inhomogeneously dispersed in AlN, is an example of such a cermet.

**Multilayers** refer to alternating layers of an optically transmitting compound with another more optically absorbing layer. Multilayering is attractive because optical properties can be engineered by the choice of individual layer thickness, while maintaining the same process (sputtering) conditions.

Similarly, the **copolymers** studied consisted of at least one transparent and an optically more absorbing phase.

In this study more than 150 chemically distinct materials were screened optically as candidates for attenuating embedded phase-shift masks. The following sections summarize the optical properties critical for DUV and 193 nm phase-shift mask design for some of the most promising candidates from the different materials classes. An overview is then given of a preliminary assessment of other mask manufacturability properties, including chemical and radiation durability, etch selectivity, alignment and inspection properties, and film stress and adhesion. We conclude with recommendations.

## 2. EXPERIMENTAL METHODS

Briefly, all of the inorganic thin film candidates were made by physical vapor deposition -- by sputtering or electron-beam evaporation. Most films were sputtered, using rf diode or magnetron methods. And most of the sputtered films were rf or dc magnetron sputtered in a cryopumped Materials Research Corp. 8667 system--- background pressure ~2x10<sup>-7</sup> Torr. Polymer films were prepared by spin coating materials in appropriate solvents (e.g., o-xylene and fluorinert FC-40 made by 3M Corp.). Substrates were Shin-Etsu quartz, 1.5" x 1.5" x 0.090" for measurement of optical properties or 5" x 5" x 0.90" for evaluation of phase-shift and optical transmission.

The optical properties of phase-shift candidates were determined from 186 to 800 nm by spectroscopic ellipsometry and UV/visible spectroscopy<sup>13</sup>. These data were combined with optical modeling<sup>14</sup> to determine the materials' optical constants<sup>15</sup> (n-ik), from which phase-shift mask designs could be calculated for DUV and 193 nm. Specifically, we used a

P. F. Carcia, R. H. French, K. Sharp, J. S. Meth, B. W. Smith, "Materials Screening for Attenuating Embedded Phase-Shift Photoblanks for DUV and 193 nm Photolithography", **16th Annual BACUS Symposium on Photomask Technology and Management, SPIE Vol. 2884**, Edited by G. V. Shelden, J. A. Reynolds, 255-63, (1996).

DUV spectroscopic ellipsometer using MgF<sub>2</sub> optics and Xenon and Deuterium combined with a Perkin Elmer Lambda 9 spectrophotometer with transmission and reflectance attachments and also xenon and deuterium lamps.

### 3. STRUCTURAL AND OPTICAL PROPERTIES

#### 3.1. AlN-CrN Composites

##### *3.1.1. Preparation and structure of AlN-CrN composites*

AlN-CrN composites with three different chemical compositions (21%, 41%, and 52% CrN) were sputtered reactively (Ar/N<sub>2</sub>) from Cr and Al targets on to a quartz substrate, held statically. The two sputtering guns were arranged in a confocal geometry, so that their sputtered fluxes overlapped at the quartz substrate, positioned about 6" from each target. The chemical composition for ~1000 Å thick films was changed by adjusting the sputtering rate from the Cr target while holding the Al-N sputtering rate constant. X-ray diffraction revealed that films richer in Al were poorly crystalline, whereas Cr-rich films had a single crystalline peak that corresponded to diffraction from planes with  $d=2.378$  Å, identical to diffraction from (111) planes of cubic CrN.

##### *3.1.2. Optical and Phase shift Properties of AlN-CrN Composites*

From variable angle spectroscopic ellipsometry and optical reflection and transmission data, the optical properties (index of refraction and extinction coefficient) were determined at 248 nm and 193 nm. Figure 1 summarizes calculated optical transmissions in AlN-CrN composites with 180° phase shift at 248 nm and 193 nm as a function of relative AlN concentration in the composite. Each point in this figure corresponds to a specific film chemical composition with a unique film thickness. These data indicate that 180° phase shift with optical transmissions of 5-10% can be achieved in AlN-CrN composites for AlN concentrations above about 50%.

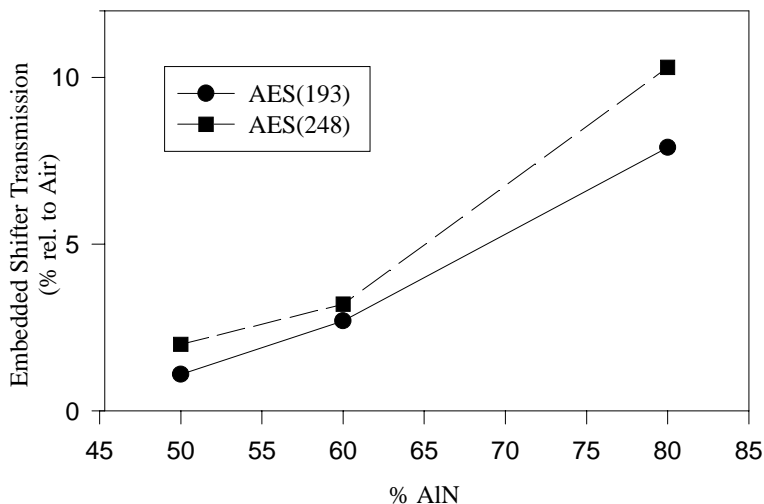


**Figure 1. Design transmission of AlN-CrN composites 193 nm and DUV attenuated embedded shifters versus % AlN.**

#### 3.2. Al-AlN Cermets

##### *3.2.1. Preparation and structure of Al-AlN Cermets*

Al/AlN cermets were made by sputtering from an Al target in an atmosphere of Ar/N<sub>2</sub>. For N<sub>2</sub> partial pressures near 20%, the extinction coefficient (k) was vanishingly small below 5 eV and then increased rapidly between 5 and 6 eV, consistent with the known band gap<sup>16,17</sup> of 6.2 eV for AlN and the presence of single phase AlN, as determined by x-ray diffraction. 13% N<sub>2</sub> marked the onset of rapid change in optical constants, precisely where the film deposition rate increased,

P. F. Carcia, R. H. French, K. Sharp, J. S. Meth, B. W. Smith, "Materials Screening for Attenuating Embedded Phase-Shift Photoblanks for DUV and 193 nm Photolithography", **16th Annual BACUS Symposium on Photomask Technology and Management, SPIE Vol. 2884**, Edited by G. V. Shelden, J. A. Reynolds, 255-63, (1996).

signaling the transition of the Al target surface from a nitrogen-saturated mode to nitrogen-deficient or more metallic mode. The formation of Al/AlN cermet in films sputtered in a smaller partial pressure of N<sub>2</sub>, reduced n and increased k at 193 nm, consistent with increasing Al content, for which n=0.1 and k=2.2. There was a similar trend at 248 nm, although n varied more slowly with N<sub>2</sub> partial pressure. And x-ray diffraction confirmed that between Al formation (%N<sub>2</sub>=0) and AlN (%N<sub>2</sub>>16%), films were comprised of a mixture of FCC Al and AlN with the hexagonal wurtzite structure.

### 3.3.2. Optical and Phase shift Properties of Al-AlN Cermets

Figure 2 and Figure 3 summarize the dependence of the 193 nm and DUV optical constants (n+ik) of Al-AlN cermets as a function of N<sub>2</sub> partial pressure during preparation. And Figure 4 shows the variation in optical transmission corresponding to 180° phase-shift designs for DUV and 193 nm, as calculated from the corresponding optical constants. Again, each point represents a unique film thickness. For 11% N<sub>2</sub>, 180° phase shift was achievable at 193 nm in a 640Å thick film with ~6% transmission, and at 248 nm in a 970Å thick film with ~12% transmission. At 193 nm 180° phase shift can be designed in this system with ~10% transmission over a wide range of synthesis conditions, whereas appropriate designs at 248 nm favor lower N-partial pressure (~10-11%).

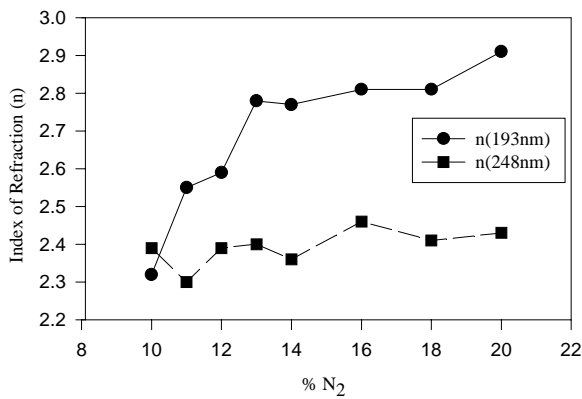


**Figure 2.** Variation of the index of refraction of Al-AlN cermets at 193 nm and 248 nm versus N<sub>2</sub> sputtering gas level.

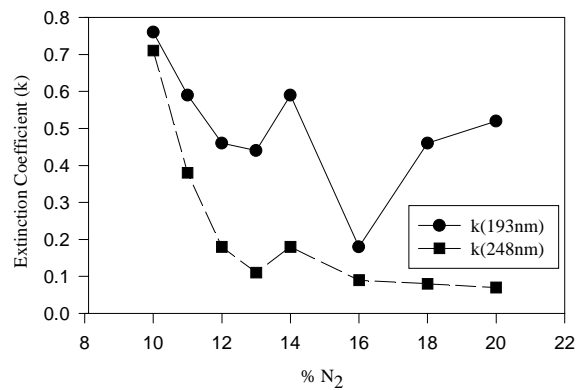


**Figure 3.** Variation of the extinction coefficient of Al-AlN cermets at 193 nm and 248 nm versus N<sub>2</sub> sputtering gas level.

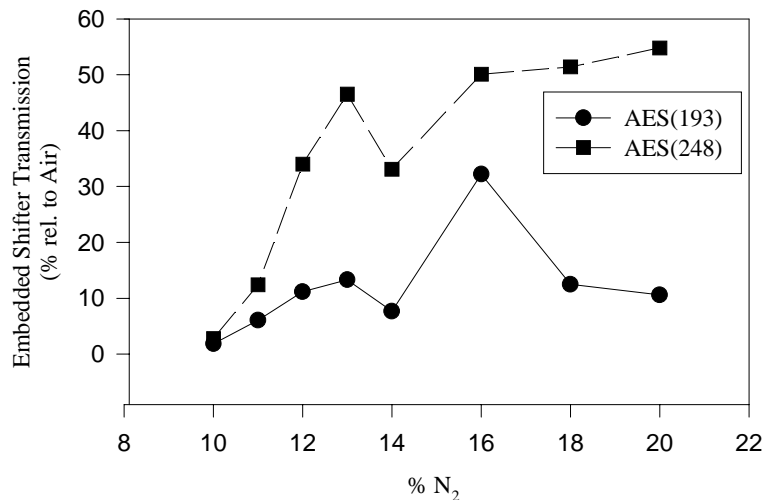


**Figure 4.** Design transmission of Al-AlN Cermet 193 nm and DUV AES versus N<sub>2</sub> sputtering gas level.

P. F. Carcia, R. H. French, K. Sharp, J. S. Meth, B. W. Smith, “Materials Screening for Attenuating Embedded Phase-Shift Photoblanks for DUV and 193 nm Photolithography”, **16th Annual BACUS Symposium on Photomask Technology and Management, SPIE Vol. 2884**, Edited by G. V. Shelden, J. A. Reynolds, 255-63, (1996).

### 3.3. $RuO_2/HfO_2$ and $CrN/AlN$ multilayers

#### 3.3.1. Preparation and structure of $RuO_2/HfO_2$ and $CrN/AlN$ multilayers

Multilayers of  $RuO_2/HfO_2$  and  $CrN/AlN$ , where  $HfO_2$  and  $AlN$  are clear and  $RuO_2$  and  $CrN$  are optically absorbing at DUV, were made by sputtering from separate metal targets in partial pressures of Ar and either  $N_2$  or  $O_2$ . The targets were physically apart so that their sputtered fluxes did not overlap. Both targets were operated in the same sputtering gas environment, although the power applied to each target, and consequently its sputtering rate, was usually different. Multilayer growth proceeded by pausing substrates on a rotatable table under each target consecutively. The chemical composition of films was adjusted by the thickness of individual layers, controlled by their deposition rates and the length of time substrates were paused under each target. Each multilayer, which was optically characterized, consisted of 20 bilayers (e.g., a bilayer refers to the thickness of one  $HfO_2$  plus one  $RuO_2$  layer) with a periodicity of 50 Å.

#### 3.3.2. Optical and phase-shift properties of $RuO_2/HfO_2$ and $CrN/AlN$ multilayers

Figures 5-8 summarize the dependence of the index of refraction and extinction coefficient on %  $RuO_2$  and %  $CrN$  in these multilayers at 248 nm and 193 nm. The general trend is to reduce  $n$  and increase  $k$  with increasing  $RuO_2$  or  $CrN$  content.

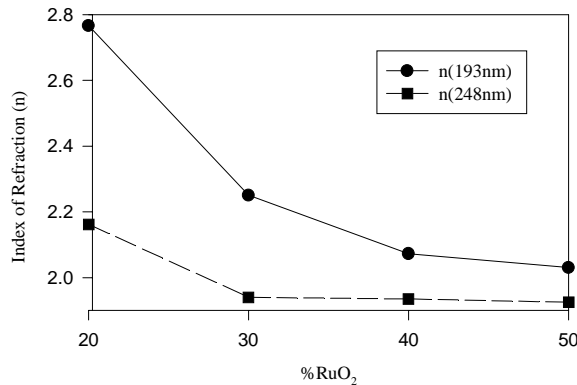


Figure 5. Variation of the index of refraction at 193 nm and 248 nm versus %  $RuO_2$  for  $RuO_2/HfO_2$  multilayers.

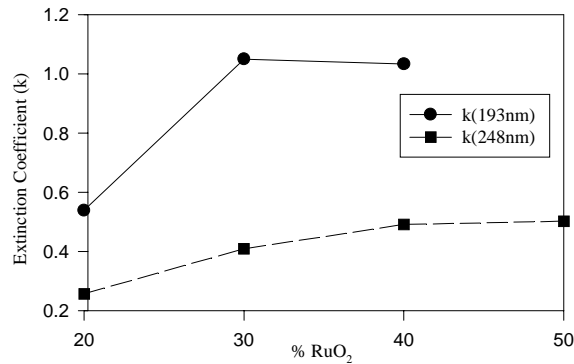


Figure 6. Variation of the extinction coefficient at 193 nm and 248 nm versus %  $RuO_2$  for  $RuO_2/HfO_2$  multilayers.

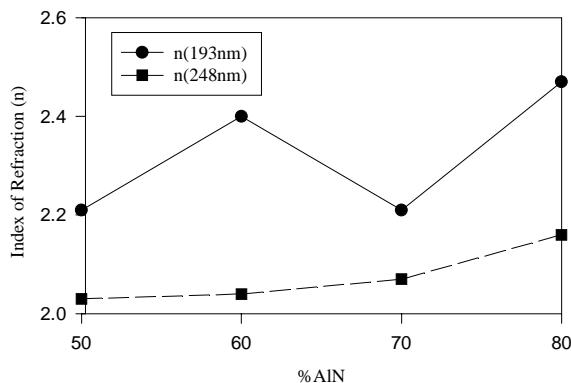


Figure 7. Variation of the index of refraction at 193 nm and 248 nm versus %  $AlN$  for  $AlN/CrN$  multilayers.

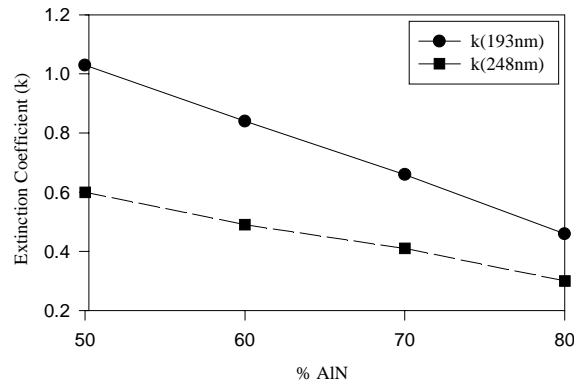
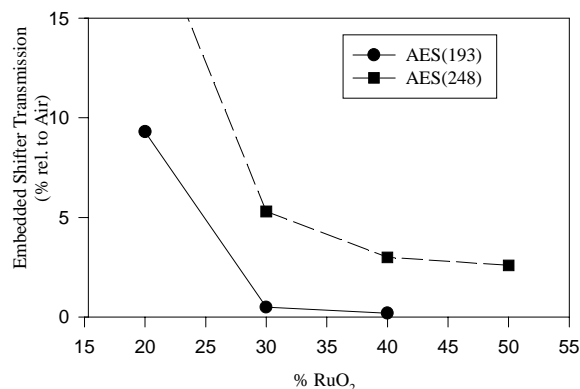


Figure 8. Variation of the extinction coefficient at 193 nm and 248 nm versus %  $AlN$  for  $AlN/CrN$  multilayers.

P. F. Carcia, R. H. French, K. Sharp, J. S. Meth, B. W. Smith, "Materials Screening for Attenuating Embedded Phase-Shift Photoblanks for DUV and 193 nm Photolithography", **16th Annual BACUS Symposium on Photomask Technology and Management, SPIE Vol. 2884**, Edited by G. V. Shelden, J. A. Reynolds, 255-63, (1996).

Figures 9 and 10 summarize the dependence of optical transmissivities, calculated for RuO<sub>2</sub>/HfO<sub>2</sub> and AlN/CrN multilayer thicknesses, corresponding to 180° phase shift at 193 nm and 248 nm on the % RuO<sub>2</sub> or % CrN. At 248 nm, acceptable transmissivities (5-12%) occur in the range 25-30% RuO<sub>2</sub>, while at 193 nm similar transmissivities occur approximately in the range ~17-25%. For AlN/CrN multilayers, 180° phase shift was also achievable in an acceptable range of optical transmission (5-10%) at both DUV (248 nm) and 193 nm. Thus both RuO<sub>2</sub>/HfO<sub>2</sub> and AlN/CrN multilayers are an ideally tunable system for attenuating phase shift masks at 248 nm and 193 nm.



**Figure 9. Design transmission of 193 nm and DUV attenuated embedded shifters versus % RuO<sub>2</sub> for RuO<sub>2</sub>/HfO<sub>2</sub> multilayers.**

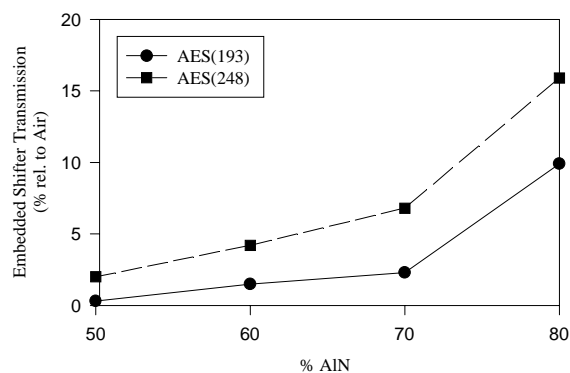


**Figure 10. Design transmission of 193 nm and DUV attenuated embedded shifters versus % AlN for AlN/CrN multilayers.**

### 3.4 Fluoropolymer and organosilicates

#### **3.4.1 Structure and optical properties of polymers**

Our AES strategy for polymers focused on the synthesis and characterization of the two basic families - fluoropolymers<sup>18</sup> and organosilicates<sup>19</sup>. The pure Teflon AF fluoropolymers are too transmissive to meet AES requirements, but could serve as a matrix for appropriate chromophores. Organosilicate polymers containing various aromatic chromophores generated a number of AES candidates. Introduction of phenyl groups into a silicate structure gave suitable materials for 193 nm AES. Replacement of phenyl by phenanthryl groups gave suitable optical properties for both 193 and 248 nm applications. Figure 11 illustrates AES designs for 248 nm and 193 nm as a function of % phenanthryl in the organosilicate. In a particularly encouraging development, by appropriate compositional tuning in a mixed phenyl-phenanthryl silicate system, AES materials with identical optical constants at both 193 and 248 nm can be obtained, whereby AES photoblanks for both wavelengths can be prepared by varying only the film thickness. The utility of these materials in photomask applications will require further careful examination of several processability issues, including dry etch characteristics, chemical and radiation durability, and film adhesion.

P. F. Carcia, R. H. French, K. Sharp, J. S. Meth, B. W. Smith, "Materials Screening for Attenuating Embedded Phase-Shift Photoblanks for DUV and 193 nm Photolithography", **16th Annual BACUS Symposium on Photomask Technology and Management, SPIE Vol. 2884**, Edited by G. V. Shelden, J. A. Reynolds, 255-63, (1996).

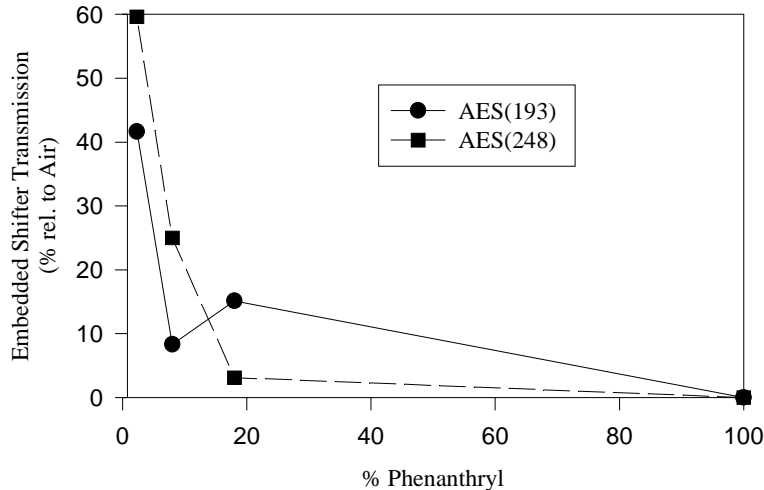


**Figure 11. AES photoblack transmission as a function of % Phenanthryl in phenanthryl silicate polymer films for both 193 nm and 248 nm lithographic wavelengths.**

#### 4. OVERVIEW OF OTHER DUV/193 nm AES PROPERTIES

##### 4.1. Dry and wet etch properties

AES candidates with either AlN or Al<sub>2</sub>O<sub>3</sub> as the optically "clear" component were readily dry etched in a Cl<sub>2</sub>/Ar plasma (58 sccm/5 sccm, 400W, 40 mTorr). Specifically, AlN/CrN multilayers etched at a rate of ~100 Å/min, under which conditions an AES mask would require less than 10 min. to etch completely. Predictably, with a Cl<sub>2</sub>-based etch, selectivity to quartz was excellent, e.g. ~10:1 for AlN/CrN multilayers. However, the selectivity to Novolac resist, commonly used for e-beam and laser fabrication of masks, was poor-- < 1:10. Not surprisingly, AES candidates based on Al compounds etched slowly (~1-5 Å/s compared to ~20 Å/s for Cr) in standard wet Cr etchants.

##### 4.2. Radiation durability at 193 nm

Selected AES candidates were exposed to a million pulses (14 ns duration with 8 mJ/cm<sup>2</sup>/pulse at 100 Hz repetition rate) of 193 nm radiation from a ArF laser (Lumonics EX700). This is equivalent to 100,000 full wafer exposures (of 100 fields) at 15-20 mJ/cm<sup>2</sup> in a 5X exposure system. The optical properties of 1.5" square, coated quartz substrates were measured by spectroscopic ellipsometry before and after radiation exposure. Although nonuniform irradiation of the sample surface prevented accurate modeling to obtain quantitative changes in optical properties, we were able to qualitatively conclude that Al-AlN and Ru-Al<sub>2</sub>O<sub>3</sub> cermet had better radiation durability than some of the multilayer structures.

##### 4.3. Chemical durability

In typical Cr mask processing, a concentrated mixture of sulfuric acid and hydrogen peroxide at 70°C is used to clean the mask and remove PBS e-beam resist. The optical properties of an opaque Cr mask are unaffected by this process. We found that a commercial solution (Nano-Strip<sup>®</sup>) of concentrated sulfuric acid with hydrogen peroxide completely etched multilayer candidates with AlN, whereas a Ru-Al<sub>2</sub>O<sub>3</sub> cermet was unaffected after immersion in solution for half an hour, and a Cr-polyethylene cermet was unaffected for two hours.

##### 4.4. Inspection and alignment transmission at 488 nm

In order to permit mask inspection and alignment at 488 nm, the optical transmission of AES candidates should be < 40%; and, while 40-50% is problematic, transmissions above 50% will not permit inspection with current tools. A general

P. F. Carcia, R. H. French, K. Sharp, J. S. Meth, B. W. Smith, "Materials Screening for Attenuating Embedded Phase-Shift Photoblanks for DUV and 193 nm Photolithography", **16th Annual BACUS Symposium on Photomask Technology and Management, SPIE Vol. 2884**, Edited by G. V. Shelden, J. A. Reynolds, 255-63, (1996).

conclusion with regard to AES candidates of this study is that an inspection transmission of <40% is achievable at 248 nm, but much more challenging for 193 nm. Specifically, Al-containing compounds with a metal-like constituent, such as MoN, CrN, RuO<sub>2</sub>, or W<sub>2</sub>N, can be designed as AES at 248 nm with an optical transmission at the inspection wavelength, 488 nm, less than 40%. However, phase-shift masks designed for 193 nm will have a higher optical transmission at inspection, because of a correspondingly smaller metallic component. To achieve a transmission of <40% at the current inspection wavelength (488 nm) in a 193 nm phase-shift mask will be quite challenging and possible in only a few candidate materials. Changing inspection to a shorter wavelength can remedy this problem of too high optical transmission for DUV and 193 nm phase-shift masks.

#### 4.5. Electrical conductivity

A mask sheet resistivity of less than 10<sup>6</sup> Ω/square is needed for e-beam writing, in order to prevent registration errors due to charging effects. This property requirement is driven by the same considerations for low optical transmission to inspect masks--the metallic content or fraction of MoN, CrN, RuO<sub>2</sub>, W<sub>2</sub>N etc. Again, adequately low resistivity designs are possible for DUV, whereas they are more challenging for 193 nm. For low metallic content (<<50%), as in 193 nm mask designs, layering separate dielectric and metallic constituents can enhance their conductivity, particularly if the outermost layer is metallic and continuous. Grading the chemical composition to include more metal content in the outer layers, if this is also consistent with a low reflectivity, is another strategy to achieve a low resistivity. Depositing a separate conducting layer on the mask is another possible strategy, but this brings added complexities in mask fabrication.

#### 4.6. Film stress and adhesion (ASTM)

The calculated tolerable stress, corresponding to a warp of less than 0.3 mm over 110 mm of a .090" thick quartz substrate, is only 36 MPa. Although we measured higher stress (2-5X) in all of the sampled AES candidates, this is not considered to be serious, because film deposition conditions can generally be adjusted to minimize internal film stresses. Also, these stresses were measured in films nearly twice as thick as they need to be for a  $\pi$ -phase-shift. Since film stress scales with thickness, actual stresses in a phase-shift mask will be smaller by a half.

Film adhesion was measured by an ASTM crosshatch tape test and results categorized by the fraction of film pulled from the substrate(5-best; 0-worst). Only the Cr-polyethylene cermets had poor adhesion, corresponding to an ASTM classification between 1B and 2B. Al-AlN and Ru-Al<sub>2</sub>O<sub>3</sub> cermets showed some loss of adhesion with a classification between 3B and 4B, while the remaining films exhibited little or no loss of adhesion, corresponding to an ASTM classification of 4B to 5B. These adhesion results are in general encouraging, because there was no extraordinary attempt, such as sputter-etching the substrate prior to film deposition, to improve adhesion other than working with clean substrates.

#### 4.7. Material Toxicity

None of the materials considered as AES candidates have any apparent toxicity issues that we uncovered. Our goal has been to restrict this study to only those materials that pose minimal environmental, safety, or health risks.

### 5. CONCLUSIONS AND RECOMMENDATIONS

The requirement for optical tunability at 248 nm and 193 nm with a single materials family has led us to evaluate two-phase materials, comprised of a transparent dielectric and an absorbing metallic component. (In principle, the same materials family can be used at both longer and shorter wavelengths too). We found that making both components either nitrides or oxides simplified the synthesis and increased process latitude, which should translate into ease in manufacturing with high yield. For the nitride system, we favor AlN as the transparent dielectric layer. Several nitrides are attractive as the absorbing component, including Cr, Mo, Nb, and W nitrides. A related and optically attractive alternative for a tunable phase-shift mask is an Al-AlN composition, made by sputtering Al in a mixed metal/dielectric mode. Of course, there is much smaller process latitude when sputtering in this mode, which is a disadvantage.

P. F. Carcia, R. H. French, K. Sharp, J. S. Meth, B. W. Smith, "Materials Screening for Attenuating Embedded Phase-Shift Photoblanks for DUV and 193 nm Photolithography", **16th Annual BACUS Symposium on Photomask Technology and Management, SPIE Vol. 2884**, Edited by G. V. Shelden, J. A. Reynolds, 255-63, (1996).

For the oxide system, we favor RuO<sub>2</sub> as the metallic, absorbing component. It is unique, because it is relatively inexpensive and is one of the very few oxides that can be synthesized with wide process latitude to have metallic properties. Transparent oxides that we would co-synthesize with RuO<sub>2</sub> include oxides of Al, Hf, and Zr.

In practice the nitride and oxide AES materials can be multilayered by reactively sputtering from separate metal targets. Optical tuning is then achieved by controlling the relative thicknesses of the transparent and the absorbing layers. Alternatively, deposition can be from individual alloy targets, with a different alloy for each wavelength. Or, more attractive may be sequential deposition from two alloy targets to produce a graded chemical composition. The relative deposition from the individual targets would control the overall chemical composition of the film for the applicable AES wavelength. This last approach is related to the process currently used to make binary Cr masks and I-line phase-shift masks<sup>6</sup>. And we have demonstrated in this program optical equivalence for chemically equivalent optical multilayers and mixtures or "alloys". Thus any result obtained for a multilayer should also work as a mixture.

We also evaluated other "manufacturability" issues in the context of current Cr blank processing. We conclude that the new materials for DUV and 193 nm will require some process changes, e.g. a shift away from concentrated H<sub>2</sub>SO<sub>4</sub> + H<sub>2</sub>O<sub>2</sub> cleaning and resist stripping, and actinic inspection and alignment for 193 nm masks.

## 6. ACKNOWLEDGMENTS

This work was partially funded by SEMATECH Contract # CMTA 001A. At DuPont thin films were made with the technical assistance of M. Reilly, while optical measurements were carried out by M. Lemon and D. Jones. The authors also thank Dr. M. Mocella at DuPont for his valuable assistance with administration of the program and sharing his expertise in reactive ion etching and Prof. R. Lane at RIT, who carried out the dry etch studies on these materials. The authors also thank Pat Gardner, SEMATECH Program Manager, and Rich Harbison and Gil Sheldon, also at SEMATECH, for their guidance.

## 7. REFERENCES

- 
- <sup>1</sup> M. D. Levenson, N. S. Viswanathan, and R. A. Simpson, "Improving resolution in photolithography with a phase-shifting mask," **IEEE Trans. on Electron Devices**, **29**, 1828 (1982).
  - <sup>2</sup> M. D. Levenson, "Extending the lifetime of optical lithography technologies with wavefront engineering," **Jpn. J. Appl. Phys.**, **33**, 6765 (1994); M. D. Levenson, "Wavefront engineering for photolithography," **Physics Today**, July 1993, 28.
  - <sup>3</sup> B. J. Lin, "Phase-shifting and other challenges in optical mask technology," **SPIE** **1496**, 54 (1990).
  - <sup>4</sup> J. C. Langston and G. T. Dao, "Extending optical lithography to 0.25 μm and below," **Solid State Technology**, March 1995, 57.
  - <sup>5</sup> K. K. Shih and D. B. Dove, "Thin film materials for the preparation of attenuating phase shift masks," **J. Vac. Sci. Technol. B**, **12**, 32 (1994).
  - <sup>6</sup> F. D. Kalk, R. H. French, H. U. Alpay, and G. Hughes, "Attenuated phase-shifting photomasks fabricated from Cr-embedded shifter blanks," **SPIE** **2254**, 64 (1994).
  - <sup>7</sup> F. D. Kalk, R. H. French, H. U. Alpay, G. Hughes, "Chromium-Based Attenuated Embedded Shifter Preproduction", **SPIE** **2322**, 299-304, (1994).
  - <sup>8</sup> B. Abeles, P. Sheng, M. D. Coutts, and Y. Arie, "Structural and electrical properties of granular metal films," **Adv. Phys.** **24**, 407 (1975).
  - <sup>9</sup> E. Kay, "Synthesis and properties of metal clusters in polymeric matrices," **Z. Phys. D-Atoms, Molecules, and Clusters** **3**, 251 (1986).
  - <sup>10</sup> O. Hunderi, "The optical properties of thin films and superlattices," **Physica A** **157**, 309 (1989).
  - <sup>11</sup> "Interpenetrating Polymer Networks", *American Chem. Soc. Advances in Chemistry* series, v. 239, D. Klemperer, L. Sperlin and L. Utracki, eds., American Chem. Soc., Washington, D. C. (1994).

P. F. Carcia, R. H. French, K. Sharp, J. S. Meth, B. W. Smith, "Materials Screening for Attenuating Embedded Phase-Shift Photoblanks for DUV and 193 nm Photolithography", **16th Annual BACUS Symposium on Photomask Technology and Management, SPIE Vol. 2884**, Edited by G. V. Sheldon, J. A. Reynolds, 255-63, (1996).

- 
- <sup>12</sup> G. Dao, G. Liu, R. Hainsey, J. Farnsworth, Y. Tokoro, S. Kawada, T. Yamamoto, N. Yoshioka, A. Chiba, and H. Morimoto, "248 nm DUV MoSiON embedded phase-shifting mask for 0.25 micrometer lithography," **Bacus Photomask News**, 11 August, 1995.
- <sup>13</sup> J. A. Woollam and P. G. Snyder, "Variable angle spectroscopic ellipsometry," in Encyclopedia of Materials Characterization, Butterworth Publishers, Greenwich, 1992.
- <sup>14</sup> B. Johs, R. H. French, F. D. Kalk, W. A. McGahan, J. A. Woollam, "Optical Analysis of Complex Multilayer Structures Using Multiple Data Types", **SPIE 2253**, 1098-1106, (1994).
- <sup>15</sup> D. E. Aspnes, "The accurate determination of optical properties by ellipsometry," in Handbook of Optical Constants of Solids, edited by Edward Palik, Academic Press, Orlando, 1985.
- <sup>16</sup> S. Loughin, R. H. French, W. Y. Ching, Y. N. Xu, G. A. Slack, "Electronic Structure of Aluminum Nitride: Theory and Experiment", **Appl. Phys. Lett.**, **63**, 9, 1182-4, (1993).
- <sup>17</sup> S. Loughin, R. H. French, "Optical Functions of Aluminum Nitride", **Properties of Group III Nitrides** edited by J. H. Edgar, Electronic Materials Information Service, INSPEC, the Institution of Electrical Engineers, London, 175-89, (1994).
- <sup>18</sup> P. R. Resnick, "The Preparation and Properties of a New Family of Amorphous Fluoropolymers: TEFLON<sup>®</sup> AF", *Mater. Res. Soc. Symp. Proc.*, Vol. 167, pages 105-10 (1990).
- <sup>19</sup> R. Baney, M. Itoh, A. Sakakibara and T. Suzuki, *Chem. Rev.* **95**, 1409 (1995).

P. F. Carcia, R. H. French, K. Sharp, J. S. Meth, B. W. Smith, "Materials Screening for Attenuating Embedded Phase-Shift Photoblanks for DUV and 193 nm Photolithography", **16th Annual BACUS Symposium on Photomask Technology and Management, SPIE Vol. 2884**, Edited by G. V. Shelden, J. A. Reynolds, 255-63, (1996).